

The Observation of Intermetallic Compound Microstructure Under Sn Whisker in Lead-free Finish

Chong-Hee Yu*

Honam Research Center, Electronics and Telecommunications Research Institute
1110-6 Oryong-dong, Buk-gu, Gwangju, 500-480, Korea

(Received June 11, 2009; Accepted June 25, 2009)

Abstract: Sn whiskers can grow from the pure Sn and high Sn-based finish and cause the electrical shorts and failures. Even with the wealth of information on whiskers, we have neither the clear understanding of whisker growth nor methods for its prevention. In this study, the whisker grain roots which connected with intermetallic layer were analyzed by high-resolution transmission electron microscopy (HR-TEM). In the Sn-Cu plated leadframe (LF) that was stored at ambient condition for 540 days, filament-shaped whiskers were grown on the Sn-plated surface and η' -Cu₆Sn₅ precipitates were widely distributed along the grain boundaries at the Sn matrix. The measured of the lattice fringes at the η' -Cu₆Sn₅ was 4.71Å at the coarse grain and 2.91Å at the fine grain. The Cu₃Sn which generates the tensile stresses was not observed. The formation of Cu₆Sn₅ precipitates and intermetallic layer were strongly related to whisker growth, but, the whisker growth tendency does not closely relate with the geometric morphology of irregularly grown intermetallic compound (IMC).

Keywords: Sn whisker, lead-free, Cu₆Sn₅, high-resolution transmission electron microscopy, focused ion beam

1. Introduction

Whiskers form from low-melting or soft metals, such as tin (Sn), zinc (Zn), lead (Pb) and cadmium (Cd). The most commonly used commercial surface finishes are based on Sn. Sn whiskers, which can grow from these Sn-based finishes cause electrical shorts and failures of electronic components. Sn-Pb alloys have been used extensively for surface finishing of electronic components because Pb was found to be effective in retarding Sn whisker growth as well as reducing production costs. Since the introduction of lead-free solder alloys, electronic manufacturers have been seeking a new surface finish technology that will prevent Sn whisker growth without containing the Pb. However, the mechanism of whisker growth has not yet been clarified.

An irregular layer of Cu₆Sn₅ (η' -phase) compound was found between the Cu and Sn-Cu finish interface, but not that of Cu₆Sn₅ (η -phase) and Cu₃Sn (ϵ -phase) compound at the ambient temperature. The formation of Cu₆Sn₅ (i.e. η and η' -phase) intermetallic generates the compressive stress with in the Sn film. To the contrary, the Cu₃Sn intermetallic growth between the Cu₆Sn₅ layer and Cu substrate decreases the compressive stress. Cu₃Sn formation decreases the volume in Sn deposit, so that the compression stresses were decreased. The growth of whiskers is believed that it was

driven by the level of compressive stresses in the Sn-Cu finish.¹⁾ Cu₃Sn grows at the same rate as Cu₆Sn₅ at high temperature, but does not occur at low temperature (i.e. below 60°C).^{2,3)} Also, η' -Cu₆Sn₅ has been verified by Auger depth profiling measurements and X-ray diffraction data on samples aged at 86°C and 150°C.^{4,5)} The principle of whisker formation is related to the low recrystallization temperature of Sn.⁶⁾ In the past, transmission electron microscopy (TEM) analyses of grain microstructure and precipitate formation examined the Sn plating on a Fe42wt%Ni substrate under temperature cycling (TC) condition,⁷⁻⁹⁾ the effect of intermetallic compound (IMC) on whisker growth for a short aging time, and the growth orientation of Sn deposit and whisker.^{10,11)} However, the IMC microstructure formation under the ambient condition for a long time, which is dependent on whisker growth, has not been studied. Consequently, the microstructure of Sn-alloys needs to be analyzed in detail. In this study, the IMC microstructure and whisker growth in Sn-Cu plated leadframe (LF) area are investigated by high-resolution (HR) TEM.

2. Experiments

The 0.1524 mm-thick stamped LF by Cu (C7025R-1/2H)

*Corresponding author
E-mail: yuch@etri.re.kr

was used. It was electroplated to a thickness of approximately $7.5\ \mu\text{m}$ with Sn-3.0wt%Cu solution. The chemical composition of the Sn-Cu solution was 50 g/L of Sn^{2+} , $0.8\pm 0.2\ \text{g/L}$ of Cu^{2+} , 330 ml/L of additive, and 270 g/L acid. The current density in the Sn-Cu solution was $30\ \text{A/dm}^2$, the plating time was 60s, and the temperature was 30°C . The plated samples were stored at ambient condition ($20\text{-}25^\circ\text{C}/30\text{-}80\%$ RH) for 540 days ($4.66\times 10^7\ \text{s}$). The morphology of the plating surface was observed by field emission scanning electron microscopy (FE-SEM). The IMC and interface microstructure under the areas with the whisker were analyzed using a TEM specimen, which was prepared by the focused ion beam (FIB, Strata 400S, FEI) technique without any mechanical damage to the observed areas. The lead-free plated LF surface was coated with a platinum (Pt) target for protecting the sample during the FIB milling process. FIB milling was performed with a Ga^+ ion source at the acceleration voltage of 30 keV to prepare a rectangular hole on the surface. Final thinning of the TEM specimen was performed by micro milling with a 100 ion beam. The oxide film was also removed using Ga^+ ion with 30 keV, 28 pA for 60s. The specimens were observed by using Tecnai G²F30S-TWIN(FEI) at the acceleration voltage of 300 keV. The IMC was analyzed by energy dispersive X-ray (EDX) microanalysis, and the electron diffraction pattern of the IMC was analyzed by JEM-2010(JEOL), as well.

3. Results and Discussion

The eutectic Sn-Cu finish contains 0.7wt% of Cu. In electroplating, it is hard to control such a low concentration of Cu precisely. If there is more Cu in the finish, the precipitation of Cu_6Sn_5 will be greater and whisker growth will be faster. On the other hand, a lesser amount of Cu may reduce whisker growth, but the solder will consume more Cu from the under-bump metallization or the bond pad.

Figure 1a shows the shape of the whisker on the Sn-Cu plated LF after storage in ambient condition for 540 days. Two filament-shaped Sn whiskers were grown on the Sn-plated surface. The lengths were approximately $18\ \mu\text{m}$ and $76\ \mu\text{m}$. The long whisker is growing from a surface nodule of large recrystallized grains. The temperature of Sn is approximately 30°C , which means that recrystallization will spontaneously occur around ambient temperature (above and below 30°C), reforming a strain-structure. This recrystallization process commonly occurs in the bright Sn finish which consisted with small sized grain less than $1\ \mu\text{m}$.⁶⁾ However, the nodule structure was not observed at the short whisker. It means that there are several different

whisker formation mechanisms (e.g. recrystallization, dislocation, IMC) according to the whisker shape, even if on the same kind of plating layer. On FeNi42 LF, the grown whiskers generally have a high density per unit area and a long length, even if the numbers of TC cycles is small. This is caused by the excessive compressive stress generated from the large difference in the coefficient of thermal expansion (CTE) between FeNi42 ($4.3\ \text{ppm}/^\circ\text{C}$) and Sn ($23.0\ \text{ppm}/^\circ\text{C}$). Thus, the relationship between whisker length and the number of TC cycles shows the parabolic curve.¹²⁾ In contrast, the IMC precipitates were widely distributed along the grain boundaries on the Sn-Cu plated Cu LF. The driving force of Sn whisker growth was due to the diffusion of Cu into the Sn to form IMC and it formed near ambient temperature was the dominant diffusing species in IMC.⁷⁾ The reaction is controlled by the release of Cu atoms from the Cu lattice. Compressive stress concentrated at the grain boundary could affect the growth of the long whisker even if during for a short period of time. Figure 1b presents the FIB micrograph showing the root of the filament-shaped whisker. It presents the overall structure of IMC particles at the Sn and Cu interface. The large IMC precipitates at grain boundary are the source of compressive stress in the Sn-Cu finish. It provides the enough driving forces for spontaneous Sn whisker growth. The grain size in the Sn matrix is approximately several microns. The

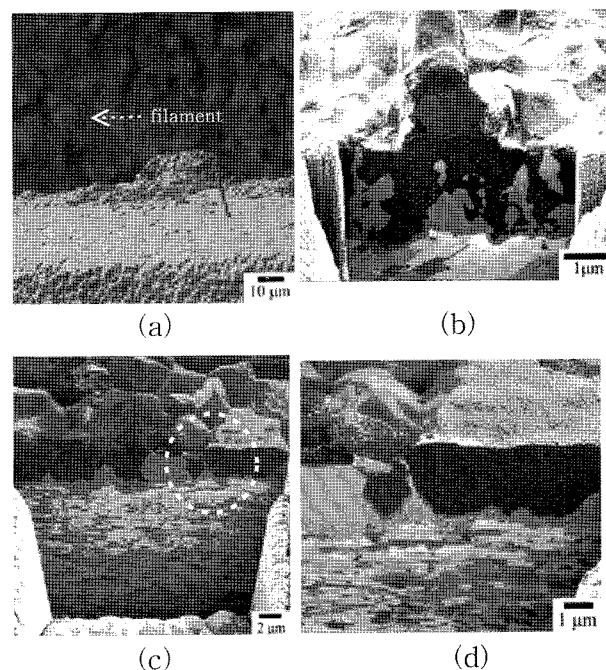


Fig. 1. Whisker grown on Sn-Cu plated LF after storage in ambient condition for 540 days. (a) SEM image; (b) FIB image of below the area which has whisker; (c) FIB image of below the area without whisker; (d) magnified image.

columnar structures which found in the pure Sn deposit were also observed in the Sn-Cu finish. Figure 1c shows the flat area with no whisker. The morphology of IMC that was grown as the flame-shaped precipitates at grain boundaries did not changed comparing with morphology at Fig 1b. Thus, the whisker growth is not closely relate with the geometric morphology of irregularly grown IMC. Some of the IMC precipitates have reached to the interface between the Sn-Cu finish and its surface oxide. Figure 1d is the magnified image which indicated by circle at Fig. 1c. Grain boundary precipitates of IMC are clearly shown.

Figure 2 shows the surface morphology after removing the oxide film under the area which has the whisker. The oxide film has irregular thickness because of the different environmental condition, and the average thickness is about several nm. The contrast depends on the degree of channeling of the ions; it appears dark when there is a high degree of channeling and it appears bright when there are more backscattered ions. IMC particles which indicated by arrow are observed at the light gray images. The polygon grain structure in the Sn matrix is clear and the IMC particles are located in the grain boundaries. Owing to the channeling effect, some of the Sn grains appear darker than other. Sn is a low melting-point metal and there are many defects in the Sn coating after plating process. The protective oxide film (SnO_x) and defects on the oxide film could be key factors in whisker formation.¹⁾ Lee¹¹⁾ suggested that there is a native and protective oxide film on the Sn surface, so that surface processes are restricted. Local stress develops because the protective oxide film limits active the diffusion such as Sn self-diffusion, hydrogen diffusion, vacancies migration, etc. A tin surface with defects in grain packing, along with pitting and pin holes, may cause defect enhanced oxidation. At local defects in the oxide film, such as grain-boundary triple points or chemical inhomogeneities, surface constraints on the diffusion of atoms or vacancies can break down. Without a surface

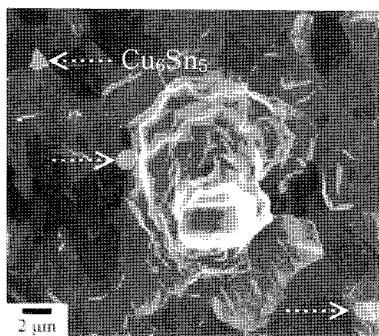


Fig. 2. An enlarged FIB image of surface area which has whisker after removing the Sn oxide.

oxide film, the internal compressive stress in Sn will be relieved uniformly over the entire Sn surface, and there will be no Sn whisker. The necessary condition of whisker growth is that the protective surface oxide must not be too thick so that it can be broken at certain weak spots on the surface. From these spots whiskers grow to relieve the stress. However, Moon *et al.*¹³⁾ reported that the whiskers were observed after removed the Sn oxide film and it implies that there is little influence of oxide film. The effect of oxide film is one of the several growth models that have been suggested to explain whisker growth.

Figure 3a shows a bright-field TEM image under the areas with whisker. The top of mountain-shaped area is a part of the filament-shaped whisker and the area indicated by circle at the top of right side is Pt plating. Randomly grown IMC precipitates were shown along the Sn grain boundaries. At the boundary between the Sn grains, IMC grew shaped like a river course. Some of the precipitates grew up to the Sn-Cu plating surface, as shown at the area which indicated by dotted. The irregular-shaped IMC layer containing the large grains was observed between the Cu and Sn interfaces. Also, the thin planar IMC layer which has the fine-grain precipitates of approximately 90-145 nm in diameter is shown. Figure 3b is the magnified image shows IMC precipitates between the Sn grains. All IMC was identified as the Cu_6Sn_5 , and no new phases were identified. Through the analyzed results by EDX, the large grains formed at the Sn matrix contained 50.7at%Sn and 49.3at%Cu. The composition of Cu was lower than that of the ideal η' - Cu_6Sn_5 (i.e. 55.2at%). However, the EDX result of an FIB-fabricated TEM specimen is only of semi-

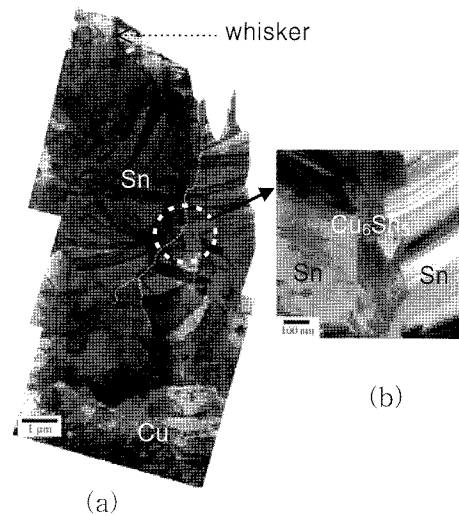


Fig. 3. Cross-sectional TEM images of the Sn whisker and Cu substrate. (a) overall image; (b) magnification image; (c)-(d) EDS mapping of the elements of Cu and Sn. The same area of specimen was analyzed.

quantitative. Thus, we can conclude that the EDX result and diffraction analysis are in a reasonable agreement with each other. The TEM observations showed that there are two concurrent mechanisms which caused the sequential formation of the η' - Cu_6Sn_5 compound: one is the interstitial transport of Cu in Sn and the other is the grain boundary diffusion of Sn in Cu. Their action between Sn and Cu occurs at ambient temperature, and it continues as long as there is a supply of Sn and Cu. Their action and the IMC formation will supply the enough a compressive stresses to keep the whiskers growing. Although η' - Cu_6Sn_5 is stored for a long time near ambient temperature, it does not transform to the η - Cu_6Sn_5 because of the kinetic constraints. Furthermore, Figure 3c-d shows the mapping result for the Cu and the Sn element of Fig. 3a, and it confirms the η' - Cu_6Sn_5 growth.

The HR-TEM images and the electron diffraction pattern show the clear lattice fringes at the interfacial layer between η' - Cu_6Sn_5 and Cu in Figure 4. Figure 4a shows the irregular-shaped Sn grain was surrounded by η' - Cu_6Sn_5 . Coarse inter metallic particles decorate the grain boundaries with finer particles with in the Sn grains. Figure 4b is the HR-TEM image which shows the indicated area by circle at Figure 4a. As shown in Fig. 4b, there was no azimuth relation between η' - Cu_6Sn_5 and Cu, which were contacted each other with tilted boundary. The measured spacing of the lattice fringes was 4.71\AA . The Kirkendall voids generated by unbalanced diffusion were not found at the interface between η' - Cu_6Sn_5 and Cu, due to the slow atomic diffusion at the ambient temperature. In general, the Kirkendall voids were generated by uneven diffusion rates between the two metals at the high temperature. Figure 4c-e present the electron diffraction patterns each area. Figure 4c shows the cubic structure (S.G.: Fm3m (225), JCPDS 4-0836) of Cu, and the measured lattice constant was $a=3.615\text{\AA}$. Figure 4d shows the tetragonal structure (S.G.: 141/amd (141), JCPDS 89-2958) of Sn, and the measured lattice constant was $a=5.8327\text{\AA}$, $c=3.1825\text{\AA}$. Figure 4e shows the monoclinic structure (S.G.: C2/c (15), JCPDS 45-1488) η' - Cu_6Sn_5 , and the measured lattice constant was $a=11.033\text{\AA}$, $b=7.294\text{\AA}$, $c=9.830\text{\AA}$. The Cu_6Sn_5 can take two different phases; one is the high-temperature stable phase η - Cu_6Sn_5 which is a hexagonal close-packed structure, and the other is the low-temperature stable phase η' - Cu_6Sn_5 phase with as upper structure type, having a phase transformation approximately in the range of 168 to 189°C .^{14,15)}

Figure 5a is the TEM photograph of the interface in contact with two kinds of grains, Cu_6Sn_5 and single Sn grain. Figure 5b shows the rectangular region denoted by

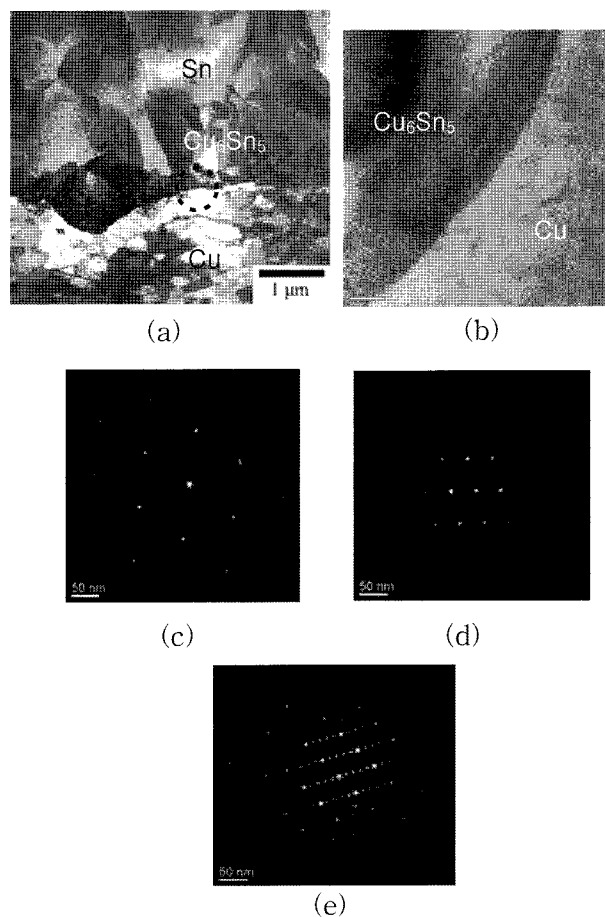


Fig. 4. (a) Cross-sectional TEM image of the Cu_6Sn_5 and Cu interfacial layer. Enlarged HR-TEM image of Fig. 3(a) is shown in Fig. 4(b) and (c)-(e) electron diffraction patterns.

Fig. 5a as "A", which was an enlarged HR-TEM image. The measured spacing of the lattice fringes was 2.91\AA . At the area pointed by arrow, Sn and η' - Cu_6Sn_5 was contacted with each other had tilted boundary. A grain boundary is the region between two grains having different lattice orientations. The measured large-angle misorientation (i.e. crystal distortion at grain boundary) is about 58 degree. The higher angle between misoriented grains has the higher the energy of the grain boundary.

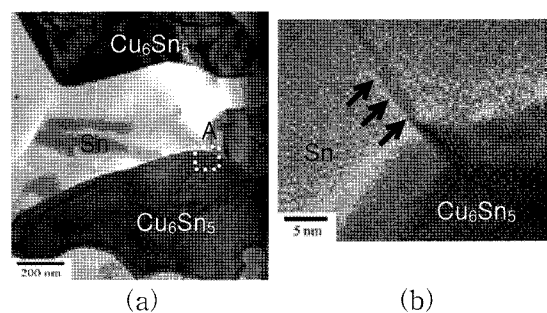


Fig. 5. (a) Cross-sectional TEM image of the Cu_6Sn_5 and Sn interfacial layer. (b) Enlarged HR-TEM image [the rectangular region denoted by "A" in Fig. 4(a)].

The formations of the precipitates and η' -Cu₆Sn₅ layer were strongly related to the whisker growth. The η' -Cu₆Sn₅ growth generated the inner compressive stresses. And these stresses accelerated the whisker growth at the weak point on the oxide layer of the Sn finish. In this study reported that, the spacing of lattice fringes has no physical meanings in the issue of whisker formation. But, the fine and coarse η' -Cu₆Sn₅ layer may generate the inner compressive stresses at the deposit layer. This topic should be investigated in future research.

4. Conclusions

The relation between intermetallic and the whisker growth under ambient condition was investigated by FIB and HR-TEM. During aging at the ambient temperature, even if on the same plating layer there are several different whisker formation mechanisms, according to the whisker shape. The main force of the whisker growth from the nodule structure grain is recrystallization, and the short filament-shaped whisker is affected by compressive stresses driven by IMC growth. Some of the IMC precipitates have reached to the interface between the Sn-Cu finish and its surface oxide. The increase of η' -Cu₆Sn₅ volume produces the compressive stress in the finish. Fine-grain η' precipitates were observed between Sn-Cu finish and Cu LF. And the coarsening of η' was existed over the fine-grain η' , as well. Both crystals (i.e. η' -Cu₆Sn₅ and Cu, η' -Cu₆Sn₅ and Sn) were contacted each other and the Kirkendall voids were not observed at the interface.

References

1. K.N. Tu, and C.J.M. Li, "Spontaneous whisker growth on lead-free solder finishes", *Mater. Sci. Eng. A*, 409, 31-139, (2005).
2. I. Sakamoto, "Whisker test methods of JEITA whisker growth mechanism for test methods", *IEEE Trans. Elect. Packag. Manuf.*, 28, 10-16, (2005).
3. K.N. Tu, "Interdiffusion and reaction in bimetallic Cu-Sn thin films", *Acta Metall.*, 21, 347-354, (1973).
4. K. Fujiwara, M. Ohtani, T. Isu and etal, "Interfacial reaction in bimetallic Sn/Cu thin films", *Thin Solid Films*, 70, 153-161, (1980).
5. R. Chopra, M. Ohring and R.S. Oswald, "Low temperature compound formation in Cu/Sn thin film couples", *Thin Solid Films*, 94, 279-288, (1982).
6. Boguslavsky and P. Bush, "Recrystallization principles applied to whisker growth in tin", In *Proc. APEX Conf.*, Anaheim, (2003).
7. G.T.T. Sheng, C.F. Hu, W.J. Choi, K.N. Tu, Y.Y. Bong, and Luu Nguyen, "Tin whiskers studied by focused ion beam imaging and transmission electron microscopy", *J. Appl. Phys.*, 92, 64-69, (2002).
8. K.S. Kim, S.W. Han, and J.M. Yang, "Behavior of tin whisker formation and growth on lead-free solder plating", *Thin Solid Films*, 504, 350-354, (2006).
9. N. Kuwano, Y. Jia, R. Tajima, S. Koga, S. Tsukamoto, and Y. Ohno, "Application of a focused ion beam mill to the characterisation of a microstructure in tin plating on a Fe 42wt% Ni substrate", *J. Electron. Microsc.*, 53, 541-544, (2004).
10. T. Kakeshita, K. Shimizu, R. Kawanaka, and T. Hasegawa, "Grain size effect of electro-plated tin coatings on whisker growth", *J. Mater. Sci.*, 17, 2560-2566, (1982).
11. B. Z. Lee, and D. N. Lee, "Spontaneous growth mechanism of tin whiskers", *Acta Mater.*, 46, 3701-3714, (1998).
12. M. Dittes, P. Oberndorff, P. Crema, and V. Schroeder, "Tin whisker formation in thermal cycling conditions", *IEEE*, Singapore, (2003).
13. K.-W. Moon, C.E. Johnson, M.E. Williams, O. Kongstein, C.A. Handwerker, and W.J. Boettinger, "Observed correlation of Sn oxide film to Sn whisker growth in Sn-Cu electrodeposit for Pb-free solders", *J. Electron. Mater.*, 34, L31-3, (2005).
14. A.K. Larsson, L. Stenberg, and S. Lidin, "The Superstructure of Domain-Twinned η' -Cu₆Sn₅", *Acta Cryst.*, 50, 636-643, (1994).
15. C.W. Hwang, J.G. Lee, K. Suganuma, and H. Mori, "Interfacial microstructure between Sn-3Ag-xBi Alloy and Cu Substrate with or without Electrolytic Ni Plating", *J. Electron. Mater.*, 32, 52-62, (2003).